# WH$_n$ under pressure

# WH$_n$ under pressure

**Patryk Zaleski-Ejgierd**[1]**, Vanessa Labet**[2]**, Timothy A Strobel**[3]**,
Roald Hoffmann**[2] **and N W Ashcroft**[1]

[1] Laboratory of Atomic and Solid State Physics and Cornell Center for Materials Research,
Cornell University, Clark Hall, Ithaca, NY 14853, USA
[2] Department of Chemistry and Chemical Biology, Baker Laboratory, Cornell University, Ithaca,
NY 14853, USA
[3] Geophysical Laboratory, Carnegie Institution of Washington, Washington, DC 20015, USA

E-mail: patryk.ze@cornell.edu and rh34@cornell.edu

## Abstract

An initial observation of the formation of WH under pressure from W gaskets surrounding
hydrogen in diamond anvil cells led to a theoretical study of tungsten hydride phases. At
$P = 1$ atm no stoichiometry is found to be stable with respect to separation into the elements,
but as the pressure is raised WH$_n$ ($n = 1$–6, 8) stoichiometries are metastable or stable. WH
and WH$_4$ are calculated to be stable at $P > 15$ GPa, WH$_2$ becomes stable at $P > 100$ GPa and
WH$_6$ at $P > 150$ GPa. In agreement with experiment, the structure computed for WH is
anti-NiAs. WH$_2$ shares with WH a hexagonal arrangement of tungsten atoms, with hydrogen
atoms occupying octahedral and tetrahedral holes. For WH$_4$ the W atoms are in a distorted fcc
arrangement. As the number of hydrogens rises, the coordination of W by H increases
correspondingly, leading to a twelve-coordinated W in WH$_6$. In WH$_8$ H$_2$ units also develop.
All of the hydrides considered should be metallic at high pressure, though the Fermi levels of
WH$_4$ and WH$_6$ lie in a deep pseudogap. Prodded by these theoretical studies, experiments
were then undertaken to seek phases other than WH, exploring a variety of experimental
conditions that would favor further reaction. Though a better preparation and characterization
of WH resulted, no higher hydrides have as yet been found.

S Online supplementary data available from stacks.iop.org/JPhysCM/24/155701/mmedia

(Some figures may appear in colour only in the online journal)

## 1. Initial observations prompting this study

This is a story that begins in experiment, moves on to theory
and then returns to experiment.

It is well known that the solubility of hydrogen in
tungsten metal is extremely small at low pressures [1]. The
heat of solution is both large and positive, and thermodynamic
calculations suggest limited room temperature solubility of
hydrogen in this refractory metal at pressures even exceeding
100 GPa [2]. Because of these characteristics, tungsten is
often used as a gasket material to seal hydrogen in diamond
anvil cells at high pressure [3]. Yet, under extreme conditions,
chemistry has a way of intruding, as we shall see.

Our first experimental observation of near-stoichiometric
WH actually originated with the studies at the Carnegie
Institution of Washington of SiH$_4$–H$_2$ mixtures under
pressure. We note, however, that near-stoichiometric WH

was reported previously in a report by Kawamura *et al* [4].
Around 7 GPa, SiH$_4$ + H$_2$ samples crystallize as an fcc
molecular compound with the stoichiometry SiH$_4$(H$_2$)$_2$ [3].
The equation of state for this compound was obtained by
compressing samples confined within symmetric diamond
anvil cells, these utilizing tungsten gasket sample chambers,
through synchrotron x-ray diffraction measurements. The fcc
structure of the SiH$_4$ units in the structure is maintained to
pressures exceeding 30 GPa; however, diffraction patterns
obtained near the gasket–sample interface reveal a series of
new diffraction peaks (figure 1(a)). At 31 GPa, these peaks
were then readily indexed to a hcp lattice with $a = 2.88(1)$ Å
and $c = 4.53(5)$ Å, in excellent agreement with parameters
reported by Kawamura *et al* [4].

This important observation suggests an interaction
between the excess molecular hydrogen and tungsten metal;
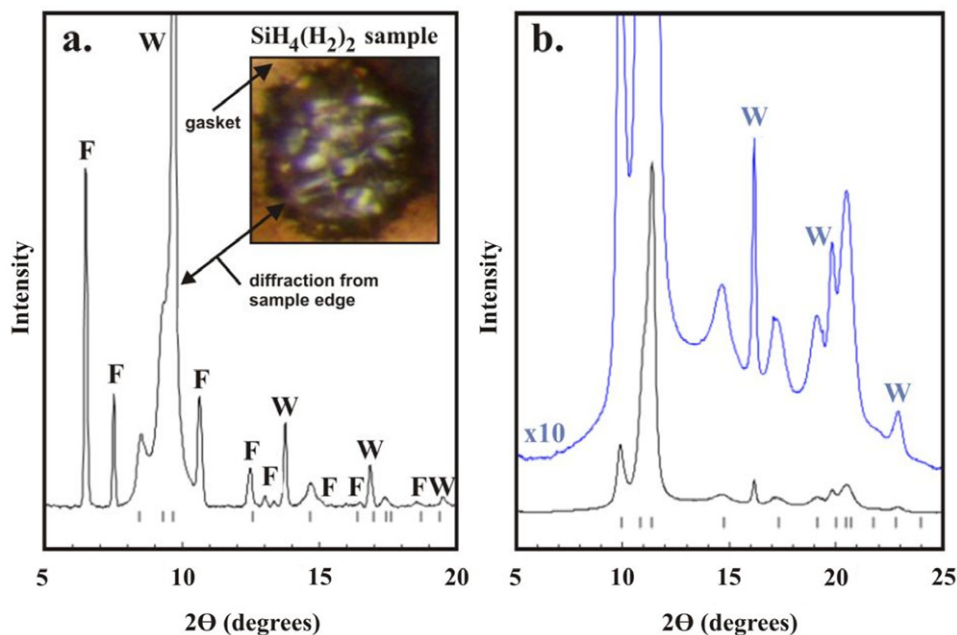that in turn motivated the present study. A correspondence

**Figure 1.** (a) Synchrotron x-ray diffraction pattern obtained from a $SiH_4(H_2)_2$ sample–gasket interface at 31 GPa. Tick marks show allowed reflections for hcp ($P6_3/mmc$) WH. Bragg peaks from fcc $SiH_4(H_2)_2$ and also the bcc W gasket are indicated by F and W, respectively. A photomicrograph of the sample is provided, where the diameter is ∼100 $\mu$m. (b) Synchrotron x-ray diffraction pattern obtained from the sample–gasket interface of Pb + $H_2$ sample at 144 ± 10 GPa. Ticks show indexing to the hcp ($P6_3/mmc$) WH structure with $a$ = 2.71(2) Å and $c$ = 4.32(3) Å.

between the observed hcp structure and similar M–H systems (e.g. Cr–H [5], Mo–H [6]) also indicates that the new phase is tungsten hydride with approximate 1:1 stoichiometry (WH), which also agrees with the report by Kawamura *et al* [4] who demonstrated the formation of ∼1:1 WH (estimated as $WH_{0.8}$ based on molar volume arguments) above 25 GPa when W powder was compressed in the presence of excess hydrogen. Kawamura *et al* [4] also suggested that WH takes up the anti-NiAs structure ($P6_3/mmc$).

The formation of tungsten hydride was rather surprising, since numerous high-pressure diamond anvil cell studies have been reported for hydrogen using tungsten gaskets, but with no mention to date of the possible presence of WH—see, for example, [7].

In addition to the $SiH_4 + H_2$ experiments, we also observed the formation of WH during experiments on Pb + $H_2$, again with a W gasket. While no structural change was observed for Pb (aside from the onset of the hcp to bcc transition above 110 GPa), strong diffraction from the sample–gasket interface again indicated the formation of WH above 30 GPa. Diffraction patterns were indexed to the anti-NiAs structure to the highest pressure measured (144 ± 10 GPa), with no evidence for a structural phase transition (figure 1(b)).

In both the $SiH_4 + H_2$ and Pb + $H_2$ experiments, hydrogen in contact with the W gasket may be viewed as a non-equilibrium system in which either hydrogen or W must diffuse through WH formed at the interface in order for significant growth of the hydride phase to occur. Ultimately, this process is dictated by chemical potential differences and the pressure gradient across the cell. The molar W:H ratio is certainly greater than one on a global basis: however, the

hydrogen concentration at the interface is very high. This large local hydrogen concentration provides some indication that the hcp WH structure is stable to at least 140 GPa, even under conditions of excess hydrogen (although kinetic barriers might well prevent the transition to a higher hydride phase).

With knowledge of these hints of the reactivity of tungsten under pressure with hydrogen, we then undertook a theoretical exploration of the structure and reactivity of tungsten–hydrogen phases.

## 2. Molecular tungsten hydrides

The extended solid state hydrides of tungsten are the focus of this study. But to set our studies in the macrocosm of tungsten chemistry with hydrogen, it is useful to review briefly what is known about discrete molecules made of tungsten and hydrogen. In fact, these molecules have attracted a great deal of attention from both the experimental and theoretical communities. The $d^0$ $WH_6$ complex, with its small ligands, is the prototypical example of a hexa-coordinated complex whose geometry is far from octahedral. This was first shown computationally by Schaefer and co-workers in 1993 [8], on the direct basis of predictions made a few years earlier by Albright, Eisenstein and co-workers for chromium hexahydride, $CrH_6$ [9]. Calculations [8, 10–12] and experiment [13, 14] agree on a distorted trigonal prism of $C_{3v}$ symmetry for the molecule $WH_6$ (see figure 2), with three equivalent W–H bonds, each 1.67 Å long and three others slightly longer at 1.72 Å.

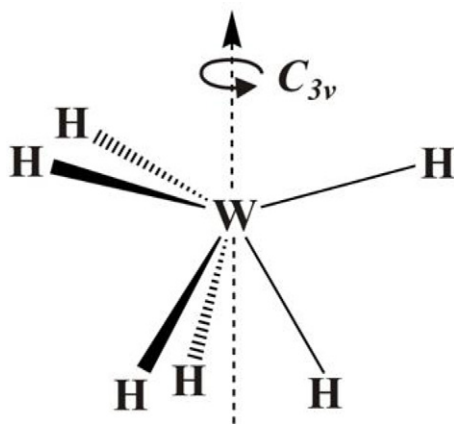In 2002 Wang and Andrews were able to synthesize the $WH_6$ molecular complex, and also to obtain evidence for

**Figure 2.** The molecular $WH_6$ complex in a distorted trigonal prismatic geometry ($C_{3v}$).

$WH_2$ and $WH_4$ as well, by reaction of laser-ablated tungsten atoms with $H_2$ during condensation in excess neon [13, 14]. The metastable $WH_6$ molecule could be characterized spectroscopically and the distorted trigonal prismatic structure then confirmed.

The neon matrix in which these studies are carried out can be maintained up to ∼12 K. Above that temperature these simple hydrides disappear in reactions into products that are not known. All of the above-mentioned hydrides are highly unstable with respect to the formation of molecular hydrogen and bulk W. The standard enthalpy of atomization of metallic W is $+203.6$ kcal mol$^{-1}$ at $T = 298.15$ K [15]. Even the most stable of the molecular hydrides, $WH_6$, has a heat of formation around $+115$ kcal mol$^{-1}$. That's a lot of driving force for decomposition.

Two years after the Wang and Andrews experiments in neon matrices, a tungsten hydride of $WH_{12}$ stoichiometry and $D_{2d}$ symmetry, involving four formal $H^-$ and four $H_2$ ligands, was predicted to be thermodynamically stable with respect to $H_2$ dissociation [16]. We may describe these molecules compactly as $WH_4(H_2)_4$. The species was also identified by Andrews *et al* in further neon matrices experiments [17]. Three more complexes of $WH_8$ and $WH_{10}$ stoichiometry, and involving $H_2$ ligands, are computed to be thermodynamically stable with respect to $H_2$ dissociation (not, however, with respect to the elements) but have not been identified experimentally so far [17].

Some 85 polynuclear molecular tungsten complexes with hydrogen bridges between at least two W centers are now known. Of these, 70 involve a single bridging H atom between two W centers, 14 involve two bridging H atoms between two W centers, and one involves a single bridging H between three W centers. Keeping in mind that scattering limitations lead to uncertainties in the W–H separations obtained from crystallographic studies, the 'normal' bond length between a tungsten metal center and a bridging hydrogen is about 1.85–1.90 Å. As will become clear below, we find just such distances in the extended structures we compute.

In a separate publication we discuss in detail the molecular tungsten hydrides and an unusual extended metastable structure of $WH_6$ stoichiometry [18].

## 3. Tungsten and tungsten hydrides in the solid state

At atmospheric pressure tungsten takes up the bcc structure (lattice constant $a = 3.16$ Å) as a high cohesive energy metal. It is only at ∼0.5–1 TPa that it is predicted to undergo a phase transformation to an fcc structure [19, 20]. There is literature on hydrogen in tungsten, and also on the surface science of tungsten, motivated in part by the possible use of tungsten in the walls of hydrogen fusion reactors [21]. The equilibrium concentration of hydrogen (atoms, hydridic in nature) in W is small at atmospheric pressure, but H atoms and ions can be forced in by high energy plasmas or ion irradiation; by quantum tunneling they then easily reach sites near defects or vacancies [22]. There is some excellent recent theoretical work on H on the surface and in the interior of W [22–24]. It should be noted that Driessen and co-workers pointed out that the hydride formation for tungsten, as for many other late transition metals, while endothermic at low pressures, becomes exothermic at high pressures [25].

While CrH (anti-NiAs structure) is known [5] and $CrH_2$ [26–28] and $CrH_3$ have been reported [29], albeit without definitive characterization, there is little information on the existence of extended solid state compounds of tungsten and hydrogen. To the best of our knowledge, apart from the previously mentioned report of WH by Kawamura *et al*, published in abstract form [4], no tungsten hydrides of any stoichiometry have been previously observed[4] or studied theoretically in the solid state, either at one atmosphere or at high pressures.

With this background on the experimental stimulus, and with the knowledge of what is known about molecular hydrides, we are ready to proceed to a discussion of the computational results on extended hydrides.

## 4. Methodology

We have examined a fairly wide range of W/H stoichiometries in extended structures and at high pressures; nine different $WH_n$ stoichiometries ($n = 1$–6, 8, 10 and 12), from WH, observed experimentally, to $WH_{12}$, the highest molecular hydride known, and by way of the appealing stoichiometry $WH_6$.

### 4.1. Searching for structures

For each stoichiometry we performed an extensive computational search for the most stable structures at 25 and 150 GPa (approximately close to the limit of normal experimental studies), combining several complementary approaches: purely random searches, evolutionary algorithms (Xtalopt [30] and USPEX [31]), and prototypical structures. In our calculations we used up to $Z = 4$ f.u./unit cell. We stress in particular that the structures we consider are all ground state arrangements (whereas the measurements are carried out at finite, close to room, temperatures).

[4] In [28] a tungsten hydride of unknown composition is mentioned.

For the purely random search, 1500 structures were generated for each W:H ratio and subsequently fully optimized. In the evolutionary approach we searched for the most stable ground state structures with the lowest enthalpy at selected pressures using XtalOpt and USPEX evolutionary algorithms [30, 31]. These approaches to crystal structure predictions are based on purely chemical composition with no experimental input required.

It has to be noted that in the cases of the $WH_{10}$ and $WH_{12}$ stoichiometries, both at 25 and 150 GPa, the most stable structures found can all be described as mixtures of $H_2$ molecules and tungsten hydrides of a lower stoichiometry (with particular emphasis on $WH_4 + xH_2$ mixtures). In the following we will focus on $WH_n$ structures but with $n = 1$–6, and 8 only.

Conveniently, for all hydrides except one, the low- and the high-pressure phases are effectively identical. We note that at pressures higher than 150 GPa more stable phases can, and do emerge, but we do not investigate those further in this work.

### 4.2. Computational details

All of the reported calculations were performed using density functional theory (DFT) with the Perdew–Burke–Ernzerhof (PBE) [32] parameterizations of the generalized gradient approximation (GGA), and as implemented in the VASP code (ver. 4.6) [33]. The projector-augmented wave (PAW) method [34] was applied with PAW pseudo-potentials taken from the VASP archive. The $1s^1$ and $5d^4 6s^2$ electrons were included in the valence space for H and W atoms, respectively. For the plane-wave basis-set expansion, an energy cutoff of 750 eV was used. The accuracy of sampling in the first Brillouin zone (FBZ) was ensured by using dense **k**-point grids resulting from a series of convergence tests. In all cases, the structures were fully optimized with respect to lattice parameters and atomic positions until the forces acting on atoms converged to 0.001 eV Å$^{-1}$ or less.

A prerequisite for the theoretical study of tungsten hydrides under pressure is that the method of calculating electronic structure used should be able to reproduce correctly the electronic structure of metallic tungsten itself. Thus we confirmed that the computational methodology described above accounts for the measured Fermi surface and associated bands in pure tungsten at one atmosphere. The agreement is very good.

Dynamical stability of the enthalpically preferred tungsten hydride structures has also been assessed through phonon analysis, within the harmonic approximation. Phonon dispersions curves were calculated using the small-displacement method as implemented in the PHON code [35]. We consistently used $2 \times 2 \times 2$ supercells in the interpolation of the force constants required for the phonon dispersion curve calculations.

### 5. Tungsten hydrides under pressure: theory

The compounds we have looked at are all on the hydrogen-rich side of the W/H phase diagram, i.e. $WH_n$, with $n = 1$–6
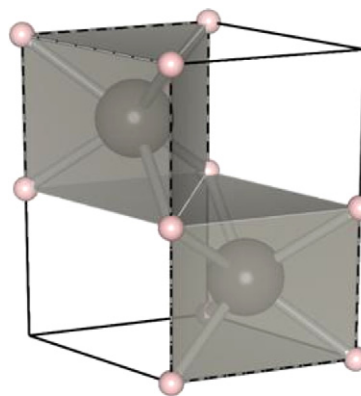


**Figure 3.** Unit cell of WH in the anti-NiAs structure (space group $P6_3/mmc$; $Z = 2$) at $P = 50$ GPa. W is gray and H pink.

and 8. First we will describe the geometrical and electronic structures of the crystal structures of lowest enthalpy found for each stoichiometry. Then we will examine their ground state stability both from the point of view of enthalpy of formation and phonon dispersion calculations.

Each stoichiometry deserves a separate discussion, but it is perhaps worthwhile to make a general observation on the coordination regularities to be expected. Obviously an increase of pressure will bring all W and H atoms closer together on average. Aside from that, since we are on the hydrogen-rich side of the phase diagram, the number of hydrogens around a tungsten atom is also likely to increase as one goes from WH to $WH_8$ at a given pressure. Also, for some particular $n$ in $WH_n$ one should begin to see $H_2$ molecules, particularly at low pressures.

Accordingly, let us now look at the structure of each tungsten hydride seriatim. We will give evidence for their stability after this survey, and eventually discuss the electronic structures of the stable phases. The three stoichiometries that yield metastable structures—$WH_3$, $WH_5$ and $WH_8$—are discussed in detail in the supplementary information (SI available at stacks.iop.org/JPhysCM/24/155701/mmedia) to this paper.

### 5.1. WH

The lowest enthalpy (ground state) structure found for the equimolar stoichiometry of tungsten and hydrogen is the anti-NiAs structure, of $P6_3/mmc$ symmetry ($Z = 2$). The unit cell for this is shown in figure 3. In this structure tungsten atoms form a hexagonal network—12 W closest neighbors—in which hydrogen atoms occupy the octahedral interstitial sites. The shortest W–W distance, 2.80 Å at $P = 50$ GPa, is slightly longer than in pure tungsten at the same pressure (2.64 Å).

Each W atom is coordinated to six H atoms in a trigonal prismatic environment and shares two hydrogen bridges with each of its 12 W closest neighbors (see figure 3). The W–H separations are all equal, proceeding from 2.07 Å at $P = 1$ atm to 1.89 Å at $P = 150$ GPa (see SI, (table S7) where is also given a histogram showing the distribution of interatomic
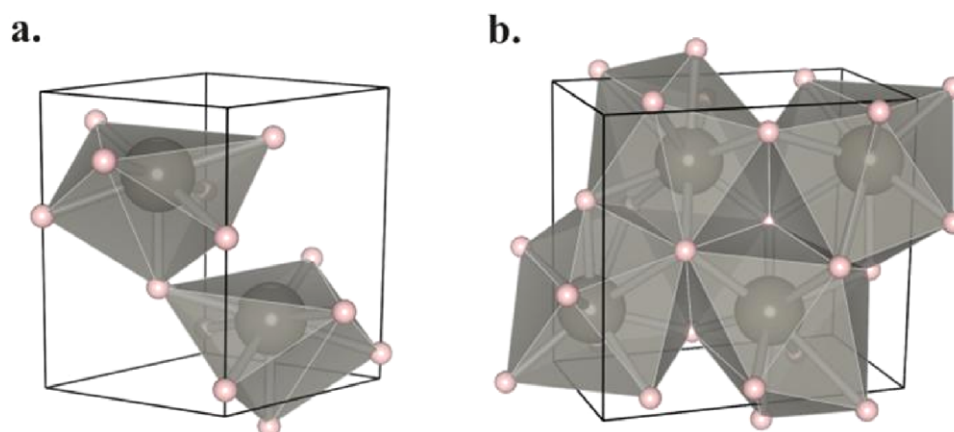
**Figure 4.** Unit cell of $WH_2$ in the *P6$_3$mc* (a) and *Pnma* (b) structures at $P = 50$ GPa ($Z = 2$ and $Z = 4$, respectively). W atoms are in gray, H atoms in pink. *P6$_3$mc* is the most stable structure for $WH_2$ below $P = 50$ GPa; *Pnma* is the most stable ground state structure between 50 and 150 GPa.

distances (figure S8) available at stacks.iop.org/JPhysCM/24/ 155701/mmedia). This separation is longer than a 'normal' W–H bond between a W metal center and a non-bridging hydride, $H^-$ ligand (1.7 Å; see, for example, [13]), but also longer than a 'normal' W–H bond between a W metal center and an $H_2$ ligand (1.8–2.0 Å; see, for example, [17]), or between a W atom and a bridging $H^-$ ligand shared with another W atom (1.8–1.9 Å). While keeping in mind the afore-mentioned unreliability of crystallographic W–H separations, this can be attributed to a larger number of W atoms between which each H atom is shared: six in the anti-NiAs structure and two in organometallic complexes.

To probe this point further, we examined the WH structures that are not favored enthalpically, for these offer a variety of coordinations of W by H. One finds in these structures that the optimal W–H bond lengths increase as the number of W atoms between which H atoms are shared increases (further details are given in the SI available at stacks. iop.org/JPhysCM/24/155701/mmedia). Interestingly, over the entire range of pressure, the NaCl structure for WH, in which W atoms are coordinated to six hydrogen atoms forming an octahedral arrangement, is about 0.18 eV/WH less stable than the anti-NiAs structure, in which the coordination sphere of W is trigonal prismatic. Note that at the molecular level, as discussed above, for $WH_6$ a $D_{3h}$ trigonal prismatic arrangement is about 4.5 eV/molecule (a very large energy) more stable than an $O_h$ octahedral geometry [8].

### 5.2. WH$_2$

In the case of $WH_2$, we find two structures competing for stability between 25 and 150 GPa. Below $P = 50$ GPa, the lowest enthalpy geometry is a hexagonal structure of *P6$_3$mc* symmetry ($Z = 2$) in which, as in WH, the W atoms form a hexagonal arrangement whose octahedral interstitial sites and half of the tetrahedral sites are occupied by H atoms. The unit cell for this is shown in figure 4(a). Because the H atoms in the octahedral sites are not located at the center of their cavities, one obtains here effectively seven-coordinated W atoms (see

the histogram in SI, figures S8 and S9 available at stacks. iop.org/JPhysCM/24/155701/mmedia). Hydrogen atoms in the tetrahedral sites are shared just among four W centers, whereas hydrogen atoms in the octahedral sites are shared among three of them only. There are either one or two hydrogen bridges between each pair of W closest neighbors.

Above $P = 50$ GPa, a ground state structure of *Pnma* symmetry ($Z = 4$) now becomes more stable than the *P6$_3$mc* structure. The corresponding unit cell is shown in figure 4(b). The *Pnma* structure involves a distorted hexagonal arrangement of tungsten atoms, as highlighted by the fact that the 12 closest W neighbors are not all exactly at the same distance (from 2.80 to 3.09 Å at $P = 50$ GPa; see SI, figure S9 available at stacks.iop.org/JPhysCM/24/155701/mmedia). The hydrogen atoms in the octahedral sites are shared among six tungsten atoms and those in tetrahedral sites among four. There are either two or three hydrogen bridges between each pair of W closest neighbors (see figure 4). In fact, the *Pnma* structure is the one adopted by most of the alkaline-earth dihydrides ($MgH_2$, $CaH_2$, $SrH_2$ and $BaH_2$). This structure has also been proposed for $WN_2$ above 34 GPa in a theoretical study a few years ago [36].

By comparing the histograms of both structures at the same pressure (see the SI; figure S6 available at stacks.iop.org/ JPhysCM/24/155701/mmedia), one finds that in the *P6$_3$mc* structure the W atoms are seven-coordinated, while in *Pnma* they are $(7 + 3)$-coordinated; the coordination sphere of W atoms can be described as tetra-capped trigonal prismatic. This increase of the coordination number of W centers as the pressure increases is in agreement with what is known about the behavior of extended systems under pressure in general [37].

We note that a $CaF_2$ structure (space group $Fm\bar{3}m$) has been reported for $CrH_2$ at ambient pressure [26, 27]. In this structure, chromium atoms form an fcc network whose tetrahedral interstitial sites are all occupied by hydrogen atoms, resulting then in eight-coordinated Cr centers. We examined this structure in the case of $WH_2$ and this also led us to look at other structures based on either a hexagonal or face-centered cubic arrangement of W atoms, with various
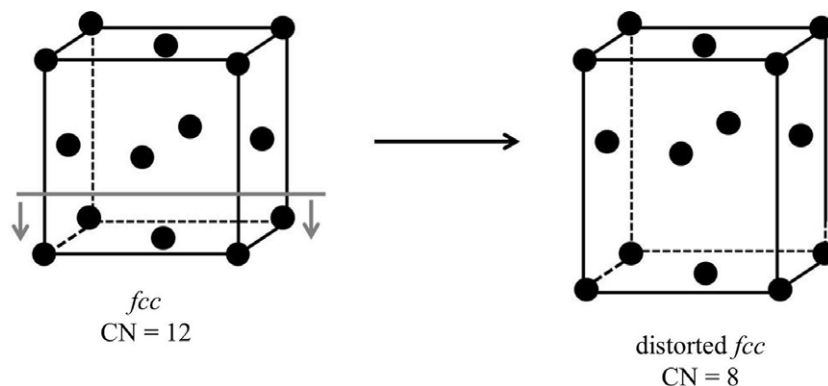
**Figure 5.** Schematic formation of the tungsten network of WH$_4$, progression from a W fcc environment.
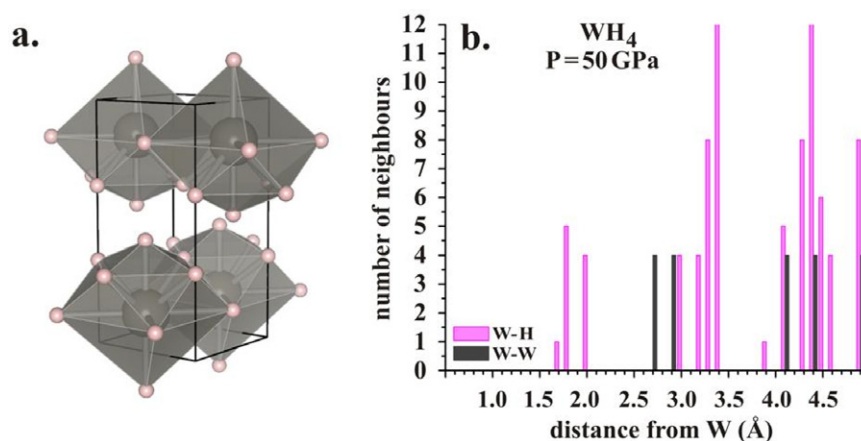


**Figure 6.** (a) Unit cell of WH$_4$ (space group $P4/nmm$; $Z = 2$) at $P = 50$ GPa. W is gray, H pink. (b) Histogram of W–H (pink) and W–W (gray) distances in WH$_4$ at $P = 50$ GPa.

occupations of the octahedral and tetrahedral sites. None of them were revealed to be lower in enthalpy than the $P6_3mc$ structure below 50 GPa and the $Pnma$ one above $P = 50$ GPa. Further details on the isomers considered and their relative enthalpy can be found in the SI (available at stacks.iop.org/JPhysCM/24/155701/mmedia).

### 5.3. WH$_4$

The best structure found for the WH$_4$ stoichiometry is derived from a distorted fcc arrangement of W atoms sketched in figure 5. In the optimum structure each W atom has eight closest W neighbors. The corresponding unit cell is shown in figure 6; it is of $P4/nmm$ symmetry, very much like one of the isomers studied for the WH$_2$ stoichiometry (see the SI, figure S1 available at stacks.iop.org/JPhysCM/24/155701/mmedia). Indeed, one can see similarities between both structures. In particular, the coordination sphere of W is the same in both cases, with ten H ligands, six of them in (pseudo)-octahedral sites and four in (pseudo)-tetrahedral sites.

The main difference between $P4/nmm$ WH$_2$ and WH$_4$ arises from the number of W atoms among which each H atom is being shared. If, in the WH$_2$ structure, the six H atoms in octahedral sites are shared among six W atoms and the four H atoms in tetrahedral sites shared among four W atoms, in the case of the WH$_4$ structure five of the six H atoms occupying octahedral sites are shared among five W atoms, the sixth one being unshared. As for the four H atoms occupying tetrahedral sites, they are shared between two W atoms only instead of four in the $P4/nmm$ WH$_2$ structure. Thus, there are either two or three hydrogen bridges between any pair of W closest neighbors. The W–H bond lengths then go from 1.73–2.18 Å at $P = 1$ atm to 1.65–1.92 Å at $P = 150$ GPa. Note that for each pressure the shortest W–H bond length is that between W centers and their unshared H ligand. At $P = 1$ atm, this W–H bond length is comparable with that computed for molecular simple hydrides (see, for example, [13]).

Note that this structure appears layered, each layer consisting of 2D sheets of WH$_4$. We will come back to this observation when we examine its electronic structure. We also note that in a partial survey of stoichiometries with high H$_2$ content, WH$_{10}$ and WH$_{12}$, we actually find mixtures of WH$_4$ and H$_2$ molecules filling the intra-sheet space, thus pulling each sheet apart.

### 5.4. WH$_6$

The best (enthalpically preferred) structure found for WH$_6$ is shown in figure 7. It belongs to the $C2/m$ space group and involves twelve-coordinated (in H) W atoms. The
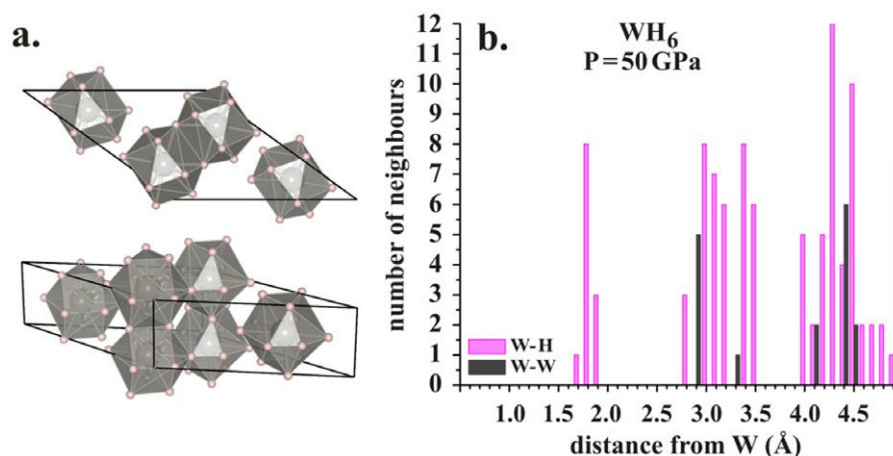
**Figure 7.** (a) Two views of the unit cell of $WH_6$ (space group $C2/m$; $Z = 4$) at $P = 50$ GPa. W = gray, H = pink. (b) Histogram of W–H (pink) and W–W (gray) distances in $WH_6$ at $P = 50$ GPa.

coordination polyhedron can be described as an equatorially hexa-capped trigonal prism. The number of W closest neighbors is now reduced to six (see the histogram; figure 7(b)), but with no simple geometrical configuration of the W network. Among the six hydrogen atoms forming the trigonal prismatic environment of each tungsten atom, two (one on each hemisphere) are shared among three W atoms and the four others among two W centers. Among the six equatorial hydrogens, four are shared between two W atoms, one by three and the last one being unshared. There are either double or triple hydrogen bridges between the W closest neighbors.

The W–H bond lengths range between 1.71–1.93 Å at $P = 25$ GPa and 1.68–1.80 Å at $P = 150$ GPa. As in the $P4/nmm$ structure for $WH_4$, the shortest W–H separation is that involving the unshared H. The structure does not survive at $P = 1$ atm. We will return later to the question of the stability of all the extended hydrides with respect to the elements.

We also investigated the stability of $WH_6$ extended structures based on aggregates of molecular $WH_6$, identified in matrix experiments [13, 14]. The details are given elsewhere [18]; briefly no molecular solids survive at any pressure. The molecular monomers spontaneously polymerize into extended structures during the optimization process.

## 6. Trends in the tungsten environment as *n* increases in $WH_n$

Now that the enthalpically preferred structure(s) found for each stoichiometry have been described, it becomes easier to examine the effect of an increase of the hydrogen content on the tungsten hydride structures. Figure 8 shows the evolution of the local environments of W atoms in the various optimum structures we found (and now we include the $WH_3$, $WH_5$ and $WH_8$ structures discussed in detail in the SI (available at stacks.iop.org/JPhysCM/24/155701/mmedia)) at the intermediate pressure of 50 GPa. In addition, the histograms relative to the W and H environments for each

stoichiometry have been gathered in the SI (figures S8 and S10 available at stacks.iop.org/JPhysCM/24/155701/mmedia).

As expected, as *n* increases in $WH_n$, the number of hydrogens around a tungsten atom at a given pressure increases: at $P = 50$ GPa it progresses from 6 in WH to 13 in $WH_8$. Simultaneously the number of W closest neighbors of W atoms decreases: from 8 + 6 in bcc-W and 12 in WH to 3 + 1 in $WH_8$. Nonetheless, the shortest W–W distance still remains remarkably constant, between 2.7 Å and 3.0 Å at $P = 50$ GPa, quite similar in fact to the shortest and second-shortest W–W distances in pure bcc-W at the same pressure—2.6 Å and 3.0 Å, respectively. No particular effect of hydrogen richness can be observed on the W–H bond length. At $P = 50$ GPa, it extends approximately from 1.7 to 2.0 Å for each stoichiometry, except WH where all W–H bonds are about 2.0 Å long.

The effect of the hydrogen content on the H–H distances is obviously larger (see the SI, figure S10 available at stacks.iop.org/JPhysCM/24/155701/mmedia). As *n* increases in $WH_n$, the shortest non-bonding H–H distance decreases. It goes from 2.3 Å in WH at $P = 50$ GPa—which is longer than a typical W–H bond—to 1.4 Å in $WH_8$ at the same pressure, which is shorter than a typical W–H bond. As a result, WH and $WH_2$ are characterized by hydrogen atoms whose closest neighbors are tungsten atoms, whereas for the other stoichiometries the closest neighbors of hydrogen atoms are other hydrogen atoms. Note that, at the same pressure of 50 GPa, the shortest non-bonding distance in the $P6_3/m$ structure for pure hydrogen is 1.7 Å [38]. In other words, as *n* increases in $WH_n$, we go from 'long' to 'short' closest non-bonding H–H distances.

## 7. Three families of tungsten hydrides

The best structures found for $WH_n$, $n = 1–6$ and 8, can be classified in three distinct groups sharing structural similarities. The first group (figure 9) gathers together $WH_1$ and $WH_2$ (both structures). Both are characterized by a hexagonal arrangement of tungsten atoms, whose octahedral
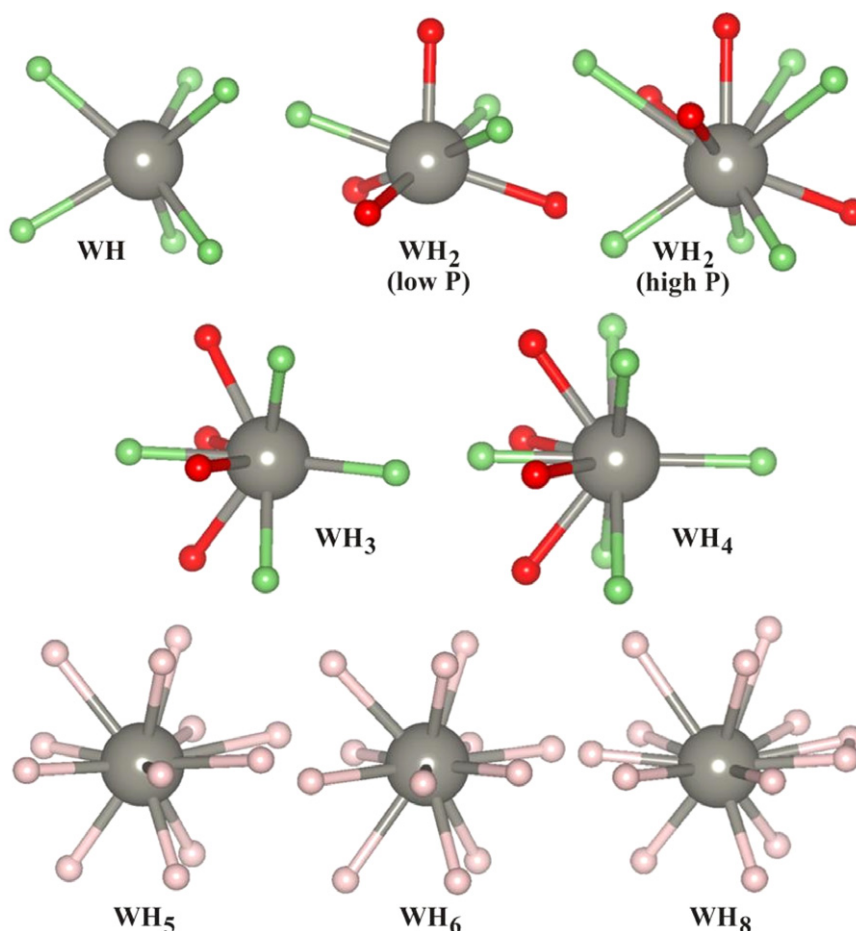
**Figure 8.** Local environment of W atoms (gray) in the $WH_n$ structures ($n = 1$–6 and 8) at $P = 50$ GPa. Note that no molecular tungsten complex is involved in these structures; in reality the hydrogen atoms (pink, red and green) are shared between several W atoms (gray). Hydrogen atoms shown in green are located in (pseudo-) octahedral interstitial sites; those in red are in (pseudo-) tetrahedral sites (see text for more information). The hydrogens in pink cannot be described as occupying interstitial positions of the tungsten network.
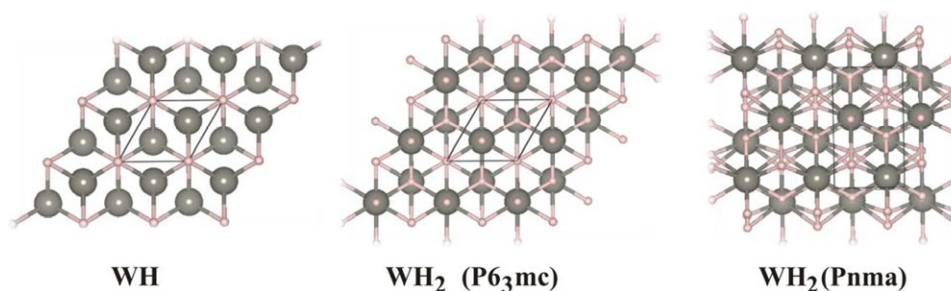


**Figure 9.** Views of the WH, $WH_2$ ($P6_3mc$) and $WH_2$ ($Pnma$) structures at $P = 50$ GPa highlighting their similarities. W are the large balls, H the small ones.

and tetrahedral interstitial sites are partially occupied by hydrogen atoms. In contrast to the other stoichiometries, in WH and $WH_2$ all hydrogens have tungsten atoms as closest neighbors. This important feature of the first group makes it possible to think of these structures as ordered stoichiometric solid solutions of hydrogen in tungsten, in which the hydrogen atoms are likely to be hydridic.

The second group—figure 10—contains $WH_3$ and $WH_4$, both characterized by a distorted fcc arrangement of W

atoms. The deformation is relatively strong, so that $WH_3$ and $WH_4$ cannot, strictly speaking, be described as interstitial. Nonetheless, it is still possible to recognize pseudo-octahedral or -tetrahedral positions of the hydrogen atoms in this tungsten arrangement. Again, note the structurally two-dimensional character of $WH_4$.

The third and last group (see figure 11) includes $WH_5$ and $WH_6$ and, to some extent, $WH_8$. One must accommodate more hydrogens into the W coordination sphere
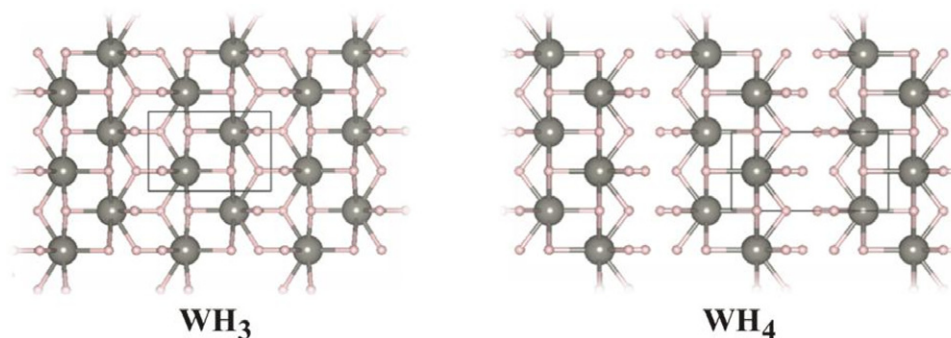
**Figure 10.** Views of the $WH_3$ and $WH_4$ structures at $P = 50$ GPa highlighting their similarities. W are the large spheres, H the smaller ones. Note the $WH_4$ slabs.
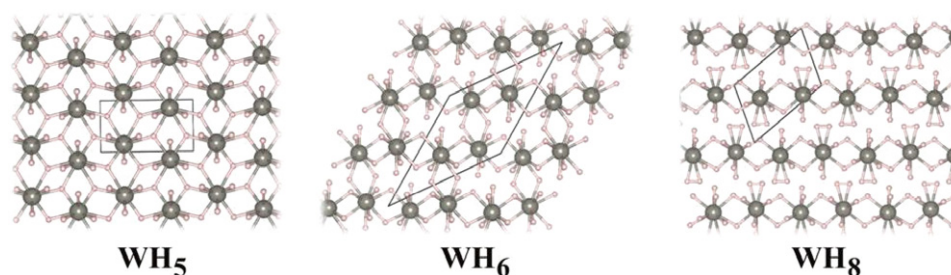


**Figure 11.** Views of the $WH_5$, $WH_6$ and $WH_8$ structures at $P = 50$ GPa highlighting their similarities. W are the large spheres, H the smaller ones.

and, accordingly, these three structures are characterized by twelve-coordination (by H of W), and a hexa-capped trigonal prismatic arrangement of hydrogens around tungstens. The place of $WH_8$ in this family is obviously special, since it is the only hydride to have $H_2$ molecular pairs coordinated with tungsten atoms.

It is remarkable to see in these figures how, within a group, the increase of hydrogen content tends to decrease the dimensionality of the tungsten network. On going from $WH_3$ to $WH_4$, the tungsten network decreases from a three-dimensional to a two-dimensional character and the number of W closest neighbors of each W atom decreases from 10 to 8. Similarly, in going from $WH_5$ to $WH_6$ to $WH_8$, the tungsten network in the equatorial plane of W atoms decreases from two-dimensional to quasi-one-dimensional and the number of W closest neighbors correspondingly decreases from 8 to 6 to 4.

It is appropriate at this point to make an observation that might, in some sense, be obvious but one that may nevertheless influence our thinking of these structures. The ratio of the atomic masses of $W:H:e^-$ is 184:1:(1/1836). (W has four stable isotopes, where $A = 184$ is the most abundant one). Born–Oppenheimer considerations allow the computation of effective interatomic potential energy curves for even light atoms, assuming the rapidly moving light electrons rapidly adjust to the nuclear motions. Given the relatively large ratio of the mass of a W atom relative to H, might our system then be a 'triply Born–Oppenheimer' one? We raise this intriguing possibility here, as we did for $PbH_4$ [39]; a separate consideration of this problem will be undertaken.

## 8. Stability of the theoretically derived structures

### 8.1. Enthalpy of formation: the tie-line plot

So far, we have searched for tungsten hydride ground state structures at several particular W:H ratios and in the 25 GPa < $P$ < 150 GPa pressure range. In order to determine which ones of those ratios (or compositions) actually belong to the W:H phase diagram at a given pressure, the ground state enthalpies of formation of the $WH_n$ ground state structures have been calculated at several pressures, with respect to pure tungsten and pure hydrogen in their most stable forms at the same pressures, i.e. bcc for tungsten and $P6_3/m$ or $C2/c$ for hydrogen [38]. The enthalpic stability of each stoichiometry was examined by plotting the enthalpies of formation per atom as a function of the hydrogen (H) molar content (see figure 12). Tungsten hydrides which are stable with respect to disproportionation into other hydrides and/or the elements are those forming a convex hull of energy with respect to composition.

At $P = 25$ GPa, and in their ground states, two tungsten hydrides appear stable with respect to the elements and other hydrides: WH and $WH_4$. By extrapolating the calculated enthalpy of formation to $P = 1$ atm, we conclude that they should both stabilize at a similar pressure of approximately 15 GPa. At $P \geq 25$ GPa, $WH_2$ and $WH_3$ are also stable with respect to disproportionation into pure tungsten and pure hydrogen but unstable with respect to disproportionation into WH and $WH_4$. As for $WH_5$, $WH_6$ and $WH_8$, they appear unstable with respect to disproportionation into the elements. Thus WH and $WH_4$ are the only two stoichiometries (among
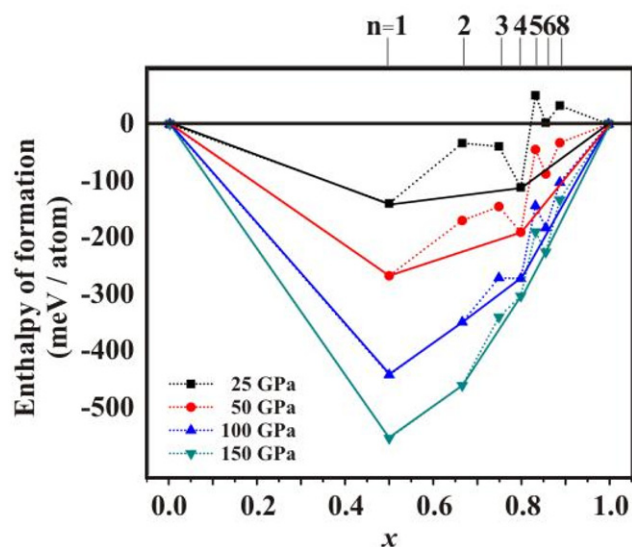
**Figure 12.** Enthalpy of formation per atom of the WH$_n$ phases with respect to their hydrogen molar content ($x = 0$ corresponds to pure tungsten; $x = 1$ to pure hydrogen) for the ground state and $P = 25$, 50, 100 and 150 GPa.

those considered in this study) predicted to exist on the H-rich side of the '$P = 25$ GPa'–W:H binary phase diagram. At equilibrium, a binary system of composition $0.5 \leq x \leq 1.0$ should result in either a mixture of WH and WH$_4$ phases if $0.5 \leq x \leq 0.8$ or a mixture of WH$_4$ and pure hydrogen phases if $0.8 \leq x \leq 1.0$.

As the pressure increases, the enthalpy of formation of each hydride becomes less and less positive and/or more and more negative, confirming that a pressure increase is indeed likely to stabilize tungsten hydrides, generally known to be unstable with respect to disproportionation into the elements at atmospheric pressure, and typically at room temperatures. At $P = 50$ GPa, all the compositions studied appear stable with respect to disproportionation into the elements. WH$_2$ becomes stable with respect to disproportionation into WH and WH$_4$ above $P = 100$ GPa and WH$_6$ stable with respect to disproportionation into WH$_4$ and H$_2$ above $P = 150$ GPa. Thus, phases of WH, WH$_2$, WH$_4$ and WH$_6$ stoichiometries are predicted to exist on the H-rich side of the '$P = 150$ GPa'–W:H binary phase diagram.

At $P = 150$ GPa WH$_3$ is still unstable with respect to disproportionation into WH$_2$ and WH$_4$, WH$_5$ unstable with respect to disproportionation into WH$_4$ and WH$_6$, and WH$_8$ unstable with respect to disproportionation into WH$_6$ and H$_2$. Nonetheless the driving force for disproportionation of WH$_3$ and WH$_8$ is remarkably low, indicating that a slight pressure increase should be enough to also stabilize those stoichiometries, contrary to WH$_5$ whose thermodynamic instability remains substantial. Although those three stoichiometries appear to be unstable with respect to disproportionation, we cannot definitely dismiss the possibility that the best structures have still not been found for them, though we are rather confident in the methodology applied so far.

Whatever pressure is chosen in the range studied (15 GPa and higher) WH certainly appears as a very stable hydride, the one for which the formation enthalpy per atom is the lowest. Thus, if one starts with pure tungsten and pure hydrogen, upon compression WH should form first and may remain stable even at highly elevated pressures. If the remaining amount of hydrogen is sufficient, it is expected to further react with WH in an exothermic reaction to form higher hydrides, WH$_2$, WH$_4$ or WH$_6$, depending on the available amount of excess hydrogen and the pressure applied. These purely enthalpic arguments do not include kinetic factors, such as the rate of diffusion of hydrogen into the WH phase, nor the possibly high potential energy barriers for reactions of WH with H$_2$. In addition, we repeat that the arguments formally apply only to ground state conditions. A further necessary caution is that the zero-point energies of the structures have not been included in the tie-line plot of figure 12 from which our conclusions are derived.

*8.2. Phonon dispersion curves (dynamical stability)*

Phonon calculations are of interest both as guarantors of dynamical stability and with respect to the information such calculations may yield on the ease or difficulty of motions in the structures considered. Two representative plots of the phonon DOS, for WH and WH$_6$, are shown in figure 13. Detailed analysis reveals that WH$_n$ ($n = 1, 2, 4, 6$) are dynamically stable at 150 GPa.

In all four cases the phonon branches separate into two groups. The high energy phonons are attributable to light hydrogen while the low energy ones arise from the much heavier tungsten atoms. It is interesting to note that, in the case of WH, the gap between the two groups of vibrations is rather wide, of the order of 1000 cm$^{-1}$. It is as if the hydrogens and the tungstens moved separately. For the higher hydrides the phonon density of states associated with hydrogen broadens substantially and eventually starts to mix with low energy tungsten branches.

The previously shown tie-line diagram (see figure 12) implies that upon decompression both WH$_4$ and WH$_6$ destabilize and eventually should decompose into a mixture of lower hydrides (most probably WH) and molecular hydrogen. As noted earlier, at $P = 1$ atm all tungsten hydrides are unstable with respect to separation into the elements. At $P < 25$ GPa significant imaginary frequencies are found in a phonon analysis, corresponding to H$_2$ elimination. In contrast to this, WH remains dynamically stable in the entire pressure range studied, an indication of the structure's robustness.

It is interesting to compare the phonon spectra of WH$_n$, $n = 1$–8, with those we computed recently for PbH$_4$ under pressure [39]. The W and Pb systems share some features: (1) a mass disparity between the heavy atoms and the hydrogens and (2) a common instability at $P = 1$ atm with respect to the elements. We did not investigate a range of stoichiometries in the Pb system, only PbH$_4$. One marked difference is that for WH$_n$ we find H$_2$ units for $n = 8$ only, whereas for PbH$_4$ we do find such H$_2$ units, albeit stretched. Indeed the H$_2$ vibrons are quite distinct in the PbH$_4$ phonon spectrum.
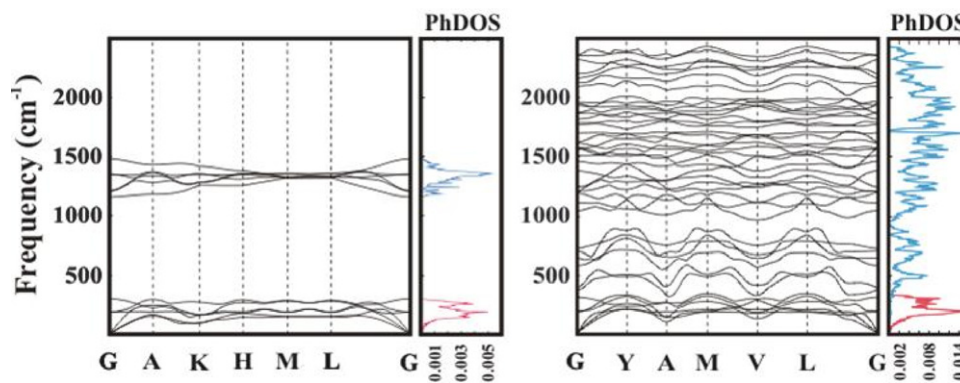
**Figure 13.** Phonon dispersions and PhDOS (states/cm$^{-1}$/cell) of WH (left) and WH$_6$ (right) at $P = 150$ GPa.

## 9. Further experimental investigation

The theoretical calculations presented in preceding sections confirm our initial experimental observations in terms of the stability of the hcp 1:1 WH structure. Yet these calculations also indicate enthalpically favorable tungsten hydride ground state structures with W:H ratios actually greater than one, e.g. WH$_4$. This may not be unexpected since our initial observations were obtained from samples formed via hydrogen interaction with the surrounding gasket material (a scenario with global composition of excess W). The calculations indicate at least the possibility for higher hydride phases in the presence of excess hydrogen and may also suggest a significant energy barrier associated with such transitions, as the local hydrogen concentration in our preliminary experiments is very large. In order to probe these possibilities, we attempted to form WH in the presence of excess hydrogen and also heated the samples to high temperatures, i.e. far beyond ground state conditions.

In a first attempt, hydrogen and some tungsten foil ($\sim$20 $\mu$m wide and $\sim$10 $\mu$m thick) were loaded into a diamond cell equipped with 200 $\mu$m culets and a tungsten gasket. The sample was compressed to 80 GPa and synchrotron x-ray diffraction patterns were then obtained. Once at 80 GPa, the tungsten foil was also heated using the two-sided IR laser heating system at HPCAT (sector 16, Advanced Photon Source). Thermal emission then collected from this sample during heating was not sufficient to accurately determine the temperature spectroradiometrically. We can only estimate the temperature to be $\leq$1000 K based on visual observation and experience with other samples.

At 9 GPa, x-ray diffraction patterns show the tungsten to remain in the bcc structure. But near 30 GPa, broad diffraction lines then appear and these are consistent with the hcp WH structure. These lines increased in intensity with pressure; however, the tungsten foil was only partially converted to WH by 80 GPa. After heating the sample ($\leq$1000 K) at 80 GPa, the W foil was almost completely converted to hcp WH. The diffraction patterns obtained after heating did not contain any new diffraction peaks and indicated the persistence of the hcp WH phase. While we attempted to load the sample with excess hydrogen, it is possible that this did not succeed at high

pressure. Some hydrogen may well have been consumed by the surrounding gasket material, for example. After heating, residual bcc W also remains present in the diffraction patterns lending credence to this suggestion (figure 14(a)).

In a final attempt to prepare higher WH$_n$ hydrides, we modified our approach by starting with fine-grained (typically $<$10 $\mu$m size) W powder and heated samples to much higher temperatures (typically up to 2200 K). In this case, the increase in surface area to volume and higher temperatures should help to alleviate kinetic hindrances. Additionally, we ensured excess hydrogen was available by only loading a few small W grains. Thus a few grains of tungsten powder (Aldrich, $>$99.99%, $d < 10$ $\mu$m) were loaded with hydrogen into diamond anvil cells using 300 $\mu$m culets and a tungsten gasket. A thin layer of LiF ($\sim$5 $\mu$m) was pressed onto each diamond before loading to act as thermal insulation in order to achieve higher temperatures and to protect the diamonds. The sample configuration is shown schematically in figure 14(b). The sample was compressed to 31 GPa and was allowed to equilibrate for two days prior to synchrotron diffraction measurements.

At 31 GPa, diffraction patterns then displayed broad lines originating from hcp WH and also a few sharp peaks from the LiF insulation layers. No bcc W metal was observed, indicating that the sample was completely converted to the hydride phase, and confirming the conditions of excess hydrogen. The sample was initially heated to $T \leq 1000$ K and quenched to room temperature for diffraction measurements. The resulting x-ray patterns revealed extremely sharp and well-resolved lines, indicating that heating had served to remove stress that might be within the WH grains. At 31 GPa, the diffraction patterns were indexed to the hcp WH structure with $a = 2.88(2)$ Å and $c = 4.60(2)$ Å, in good agreement with WH calculations at 25 GPa ($a = 2.87$ Å and $c = 4.64$ Å). No other structure was observed experimentally.

In an attempt to overcome any possible activation energy barriers associated with transitions to higher hydrides, the WH sample was heated to successively higher temperatures and then quenched (to room temperature, i.e. 300 K) between each heating for diffraction measurements. The highest temperature achieved was 2200 K and still no departure from the hcp structure was observed (figure 14(b)).
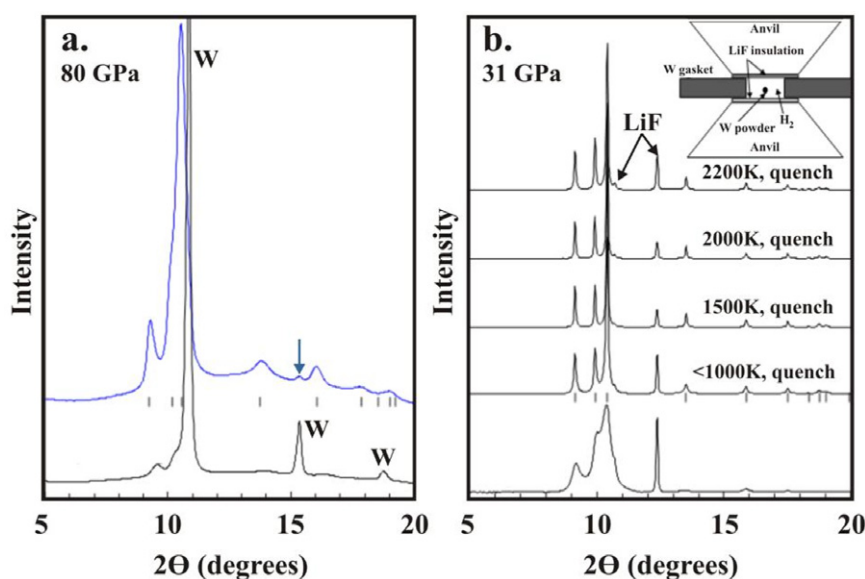
**Figure 14.** (a) Synchrotron x-ray diffraction pattern of $W + H_2$ sample (W foil) at 80 GPa before and after heating to $T < 1000$ K. Prior to heating, the sample is only partially converted to WH. After heating, the sample is almost completely converted to WH; however, some residual bcc W remains as indicated by the arrow. Tick marks indicate indexing to the $P6_3/mmc$ structure with $a = 2.85(1)$ Å and $c = 4.49(2)$ Å. (b) Synchrotron x-ray diffraction patterns obtained from WH sample (from W powder) at 31 GPa before and after heating (to $\leq 1000$ K). Heating was repeated to successively higher temperatures and quenched to room temperature for diffraction measurements. Tick marks indicate allowed reflections for the $P6_3/mmc$ structure: $a = 2.88(2)$ Å, $c = 4.60(2)$ Å. The inset shows the experimental configuration. Diffraction peaks from LiF are also indicated.

The experimental absence of a $WH_4$ phase, so clearly predicted by theory as a possibly competitive ground state structure in the pressure range experimentally accessed, is intriguing. An explanation has probably to be looked for either in the kinetics of the reaction or in the associated entropics. WH is an interstitial solid solution of hydrogen into tungsten. Its formation from bcc-W requires prior dissociation of hydrogen molecules at the surface of the tungsten sample, then diffusion of the resulting hydrogen atoms into bcc-W, and finally slight distortion of the W network to form a hexagonal arrangement. The $WH_4$ stoichiometry corresponds to a hydrogen content far above the limit of dissolution of hydrogen into tungsten (or WH). The formation of $WH_4$ from WH requires substantial modification of the tungsten network, likely associated with high energy barriers, though partly compensated by the concomitant formation of new W–H interactions, mainly ionic. Even at elevated temperatures the energy provided may be too low for the reaction to occur. If this reasoning is valid, formation of $WH_4$, predicted by theory to have a substantial range of stability in the ground state, may have to be examined from another starting point.

The reason for the absence of $WH_4$ might also be looked for in consideration of the entropy changes in the formation reaction. Indeed, the experiments performed in this work are conducted at relatively high temperatures, at least higher than 300 K. In such conditions, the thermodynamic potential for the binary system is the Gibbs energy $G$, $G = H - TS$, with $H$ the enthalpy and $S$ the entropy. So to examine the stability of a given stoichiometry, rather than plotting the formation enthalpy per atom versus the composition such as we did in figure 12, one should instead plot the formation Gibbs energy per atom (versus the composition). Our computations model

in a reasonable way the ground state conditions and allow the evaluation of enthalpy changes, $\Delta H$. To access the Gibbs energy, we also need to take into account the entropy change in a reaction, $\Delta S$. A precise estimation of the entropy of each phase is out of our reach at present.

Nonetheless we can present a qualitative argument for the sign of the entropy change in a putative formation reaction of $WH_4$. The entropy of a system is, of course, a measure of the disorder in it; the higher the number of configurations achievable by the system, the greater its entropy. The formation of a three-dimensionally polymeric and ordered tungsten hydride from tungsten metal and pure hydrogen molecules must be disfavored entropically. As the entropy rises, the more $H_2$ molecules need to be 'immobilized.' Clearly 0.25 $H_2$ molecules per atom is needed to form WH from W and $H_2$ ($\frac{1}{2}W + \frac{1}{4}H_2 \rightarrow \frac{1}{2}WH$), whereas 0.30 $H_2$ molecules per atom is needed to form $WH_4$ from WH and $H_2$ ($\frac{1}{5}WH + \frac{3}{10}H_2 \rightarrow \frac{1}{5}WH_4$). Thus the formation of $WH_4$ is likely to be more disfavored entropically than that of WH. Another qualitative argument is given by the magnitude of the entropy change needed so that the corresponding Gibbs energy change $\Delta G$ for the reaction of formation of $WH_4$ from WH and $H_2$ becomes positive. For $WH + \frac{3}{2}H_2 \rightarrow WH_4$, the enthalpy change $\Delta H$ is $-0.27$ eV/atom or $-26$ kJ mol$^{-1}$. At 300 K, an entropy change of $\Delta S = 0.09$ J mol$^{-1}$ K$^{-1}$ is then sufficient to render the Gibbs energy of the reaction positive, i.e. disfavored in the direction of the formation of $WH_4$. From a purely entropic point of view, to improve the chances of obtaining $WH_4$ from WH and $H_2$, the temperature should be lowered. But at the same time we require an elevation of temperature simply to overcome the activation barrier for the
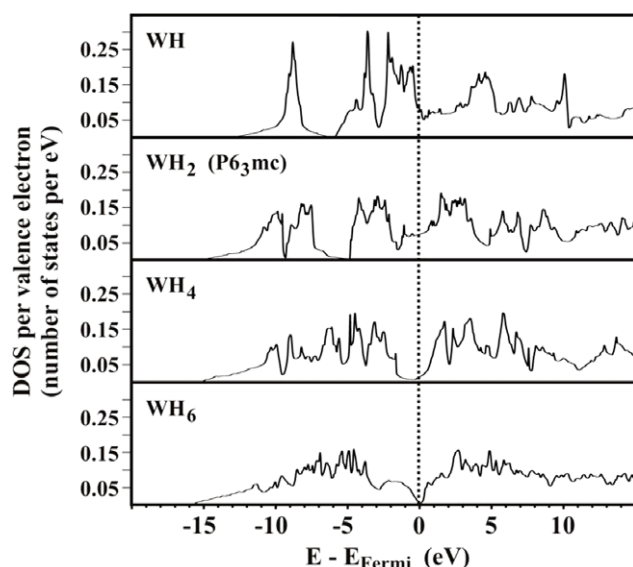
**Figure 15.** Density of states (DOS) per valence electron of WH, WH$_2$ (*P6$_3$mc*), WH$_4$ and WH$_6$ at $P = 50$ GPa.

reaction. Thus variations in temperature affect the reaction in opposing ways; it is difficult to estimate whether we have yet achieved the optimum conditions for WH$_n$ formation, $n > 1$.

A final comment concerns the early stages of the contact of tungsten with highly compressed hydrogen, an environment which is more polarizable than one imagines. The point is that, while in WH$_n$ we have considered $n$ to be relatively small ($n = 1$–12), there is clearly another very interesting limit, that of large $n$, connected to the possible dissolution of tungsten (and indeed any gasket metal) in the initiating stages of experiment into dense hydrogen, and we emphasize 'dense'. Here the rate of an ensuing transport into the hydrogen will possibly be limited by the timescale of the experiment, but the issue is not without possible importance in the suggested role of impurities (particularly transition metal impurities) in accelerating the insulator–metal transition in dense hydrogen itself [40]. High pressure diamond anvil experiments on hydrogen routinely utilize refractory metals for gasket sample chambers. Our results clearly demonstrate the formation of WH under high pressure conditions and experimentalists should be aware of this possible mechanism to deplete of the sample of hydrogen, or influence results via chemical interaction, or through the metallicity of WH.

## 10. Electronic structures

To complete the description of the tungsten hydrides initiated above, we calculate band structures and densities of states for the optimized ground state structures. Keeping in mind that the Kohn–Sham formulation of DFT is well known to underestimate the width of electronic bandgaps, the study of the electronic structures is still likely to give us information about the insulating/semiconducting/metallic character of the WH$_n$ phases. The band structures are given in detail in the SI (figures S11–13 available at stacks.iop.org/JPhysCM/24/ 155701/mmedia); figure 15 presents the densities of states

calculated at a single pressure, $P = 50$ GPa, for the four stable hydrides: WH, WH$_2$, WH$_4$ and WH$_6$.

For WH, in the entire pressure range considered (from $P = 1$ atm to $P = 150$ GPa), we observe no bandgap. Analysis of the DOS spectrum and band structure indicates high accumulation of occupied states at the Fermi level, indicative of metallic character. This is not a surprise, since W in WH is formally W in oxidation state $+$I, d$^5$. Interestingly, the electronic structure essentially does not change with external pressure. This is consistent with a relatively small change in the Wigner–Seitz radius, from $r_s = 1.60$ at $P = 1$ atm to $r_s = 1.46$ at $P = 150$ GPa. Even at the lowest pressures considered, the density of states at $E_f$ is surprisingly high for a binary hydride. Besides, there is a bandgap at two electrons per formula unit, which is likely to separate the hydridic (H$^-$) and the W 5d states.

For WH$_2$ (*Pnma*) as for WH, there is again no bandgap at the Fermi level, and still a substantial density of states. Interestingly, there is a bandgap at half occupation of the valence levels, i.e. four electrons per formula unit, which again probably separates hydridic and W 5d states.

For WH$_3$ and WH$_5$ there is also no bandgap at the Fermi level (see the SI, figures S12 and S13 available at stacks.iop.org/JPhysCM/24/155701/mmedia) whereas WH$_4$, WH$_6$ and WH$_8$, show clear depletion of density of states near/at the Fermi level in a deep pseudogap, indicating that the three latter hydrides should be considered as weak metals at best. These are ground state properties. At low pressures, WH$_6$ and WH$_8$, which are highly unstable with respect to disproportionation into WH$_4$ and H$_2$, release spontaneously H$_2$ molecules, *in silico*. Thus the pressure dependence of this pseudogap could not be studied.

Earlier in the paper, we mentioned the layered character of the WH$_4$ structure, based on geometrical criteria (see figures 6 and 10). The electronic picture given by the density of states at $P = 50$ GPa, with no clear step-like character at the bottom of the occupied band, invites one to moderate the previous statement: WH$_4$ is not as profoundly layered as we first thought . . . at least at $P = 50$ GPa. This point is illustrated further in the SI (available at stacks.iop.org/ JPhysCM/24/155701/mmedia) where the density of states of WH$_4$ at $P = 1$ atm, at $P = 50$ GPa and that of a 2D layer of WH$_4$ cut from the optimal configuration at $P = 50$ GPa are compared (see the SI, figure S14 available at stacks.iop.org/ JPhysCM/24/155701/mmedia). It appears quite clearly that the density of states of WH$_4$ at $P = 1$ atm (where it is not stable), contrary to that at $P = 50$ GPa, is characteristic of a 2D material. It is also interesting to note that the deep pseudogap present at $P = 50$ GPa does not widen at lower pressures.

In general, we would expect formal oxidation of W in WH$_n$, i.e. W$^{n+}$(H$^-$)$_n$. The hydridic states would then be expected to lie lower in energy than the W states. So at the Fermi level, the dominance of W states should decrease with $n$. While there are problems with decompositions of the total density of states in VASP, the software we use, this trend is generally confirmed. The presence of a bandgap at the Fermi level in WH$_6$, persisting as pressure is increased,

is consistent with a $(W^{6+})(H^-)_6$ formalism; the $H^-$ bands occupied and separated from the unoccupied W 5d states. The same explanation holds for the bandgap at two electrons per formula unit in WH, and at four electrons per formula unit in $WH_2$. The gap/pseudogap for $WH_4$ is therefore harder to explain.

## 11. Conclusion

Theoretical and experimental collaboration on compressed tungsten hydrides began with an experimental observation of chemistry at work when tungsten gaskets in DAC studies were pressurized. The identification of stoichiometric WH in such studies (also reported earlier by Kawamura *et al* [4]), crystallizing in the anti-NiAs structure, led to theoretical studies of a range of $WH_n$ stoichiometries, $n = 1$–6 and 8, under pressure. No phase was calculated to be thermodynamically stable with respect to separation into the elements at $P = 1$ atm, but at higher pressures a variety of stoichiometries, especially WH, $WH_2$, $WH_4$ and $WH_6$, were stabilized. They include WH and $WH_4$ from $\sim$15 GPa on, $WH_2$ at $P > 100$ GPa and $WH_6$ at $P > 150$ GPa.

The WH structure is the experimentally observed one; $WH_2$ shares with WH a hexagonal arrangement of tungsten atoms, in which octahedral and tetrahedral holes are occupied by hydrides. $WH_4$ has a strongly distorted fcc W network, with layered character. $WH_6$, for which a molecular analog exists in matrix isolation studies, is not molecular, but an extended structure that is twelve-coordinate at W. As the number of hydrogens rises, the coordination number of W (by H's) rises, with doubly and triply bridging hydrides. All of the hydrides are expected to be metallic under pressure, though the Fermi level of $WH_4$ and $WH_6$ resides in a deep pseudogap.

The computations agree with experiment on the stability under pressure of WH, but also imply that exothermic reactions to form the higher hydrides might well be expected. This theoretical result then impelled further experimental investigation of the system, introducing the W in various forms into the reaction, and heating the reactants. No other hydride was formed. Explanations are looked for in kinetic barriers to compound formation, but also in the role of entropy which, at relatively high temperatures such as those involved in the experiments, is likely to work against the consumption of $H_2$ molecules to form extended tungsten hydrides. Indeed, it is important to realize that the experimental conditions ($T > 300$ K at least) are quite far from the ground state conditions ($T \to 0$ K) modeled in our computations. But perhaps it's best for now to leave this disagreement between theory and experiment as a mystery, awaiting future resolution.

## References

[1] Arnoult W J and McMellan R B 1973 *Acta Metall.* **21** 1397
[2] Fukai Y 2005 *The Metal–Hydrogen System: Basic Bulk Properties* 2nd edn (Berlin: Springer) p 119
[3] Strobel T A, Somayazulu M and Hemley R J 2009 *Phys. Rev. Lett.* **103** 065701
[4] Kawamura H, Moriwaki T, Akahama Y and Takemura K 2005 *Proc. of Joint 20th AIRAPT–43rd EHPRG Int. Conf. on High Pressure Science and Technology (Karlsruhe, 2005)* unpublished
[5] Albrecht G, Doenitz F-D, Kleinstruck K and Betzl M 1963 *Phys. Status Solidi* **3** K249
[6] Somenkov V A, Glazkov V P, Irodova A V and Shilstein S Sh 1987 *J. Less-Common Met.* **129** 171
[7] Narayana C, Luo H, Orloff J and Ruoff A L 1998 *Nature* **393** 46
[8] Shen M, Schaefer H F III and Patridge H J 1993 *J. Chem. Phys.* **98** 508
[9] Kang S K, Albright T A and Eisenstein O 1989 *Inorg. Chem.* **28** 1611
[10] Jonas V, Frenking G and Gauss J 1992 *Chem. Phys. Lett.* **194** 109
[11] Kaupp M 1996 *J. Am. Chem. Soc.* **118** 3018
[12] Haaland A, Hammel A, Rypdal K and Volden H V 1990 *J. Am. Chem. Soc.* **112** 4547
[13] Wang X and Andrews L 2002 *J. Phys. Chem.* A **106** 6720
[14] Wang X and Andrews L 2002 *J. Am. Chem. Soc.* **124** 5636
[15] Chase M W J 1998 NIST-JANAF thermochemical tables, fourth edition *J. Phys. Chem. Ref. Data, Monograph* **9** 1
[16] Gagliardi L and Pyykko P 2004 *J. Am. Chem. Soc.* **126** 15014
[17] Wang X, Andrews L, Infante I and Gagliardi L 2008 *J. Am. Chem. Soc.* **130** 1972
[18] Labet V, Hoffmann R and Ashcroft N W 2011 *New. J. Chem.* **35** 2349
[19] Einarsdotter K, Sadigh B, Grimvall G and Ozoliņš V 1997 *Phys. Rev. Lett.* **79** 2073
[20] Ruoff A L, Rodriguez C O and Christensen N E 1998 *Phys. Rev.* B **58** 2998
[21] Bolt H, Barabash V, Krauss W, Linke J, Neu R, Suzuki S, Yoshida N and ASDEX upgrade team 2004 *J. Nucl. Mater.* **329–333** 66
[22] Heinola K 2010 *PhD Dissertation* University of Helsinki https://helda.helsinki.fi/handle/10138/23282, '*Multiscale study on hydrogen mobility in metallic fusion divertor materials*', has a very good summary of the experimental theoretical work in the field
See also Henriksson K O E, Nordlund K, Krasheninnikov A and Keinonen J 2006 *Fusion Sci. Technol.* **50** 43

[23] Johnson D F and Carter E A 2010 *J. Mater. Res.* **25** 315
[24] Heinola K and Ahlgren T 2010 *J. Appl. Phys.* **107** 113531
[25] Driessen A, Sänger P, Hemmes H and Griessen R 1990
　　 *J. Phys.: Condens. Matter* **2** 9797
[26] Snavely C A 1947 *Trans. Electrochem. Soc.* **92** 537
[27] Snavely C A and Vaughan D A 1949 *J. Am. Chem. Soc.* **71** 313
[28] Venkatraman M and Neumann J P 1991 *J. Phase. Equilib.*
　　 **12** 672
[29] Weischselfelder T and Thiede B 1926 *Justus Liebigs Ann.*
　　 *Chem.* **447** 64
[30] Lonie D C and Zurek E 2011 *Comput. Phys. Commun.*
　　 **182** 372
[31] Oganov A R and Glass C W 2006 *J. Chem. Phys.* **124** 244704
　　 Glass C W, Oganov A R and Hansen N 2006 *Comput. Phys.*
　　　 *Commun.* **175** 713
　　 Oganov A R, Glass C W and Ono S 2006 *Earth Planet. Sci.*
　　　 *Lett.* **241** 95

[32] Perdew J P, Burke K and Ernzerhof M 1996 *Phys. Rev. Lett.*
　　 **77** 3865
　　 Perdew J P, Burke K and Ernzerhof M 1997 *Phys. Rev. Lett.*
　　 **78** 1396
[33] Kresse G and Furthmüller J 1996 *Comput. Mater. Sci.* **6** 15
　　 Kresse G and Furthmüller J 1996 *Phys. Rev.* B **54** 11169
[34] Blöchl P E 1994 *Phys. Rev.* B **50** 17953
　　 Kresse G and Joubert D 1999 *Phys. Rev.* B **59** 1758
[35] Alfè D 2009 *Comput. Phys. Commun.* **180** 2622
[36] Kroll P, Schröter T and Peters M 2005 *Angew. Chem. Int. Edn*
　　 **44** 4249
[37] Grochala W, Hoffmann R, Feng J and Ashcroft N W 2007
　　 *Angew. Chem. Int. Edn* **46** 3620
[38] Pickard C J and Needs R J 2007 *Nature Phys.* **3** 473
[39] Zaleski-Ejgierd P, Hoffmann R and Ashcroft N W 2011 *Phys.*
　　 *Rev. Lett.* **107** 037002
[40] Carlsson A E and Ashcroft N W 1983 *Phys. Rev. Lett.* **50** 1305